Photocatalysis

Deutsche Ausgabe: DOI: 10.1002/ange.201501532
Internationale Ausgabe: DOI: 10.1002/anie.201501532

Extraordinary Changes in the Electronic Structure and Properties of CdS and ZnS by Anionic Substitution: Cosubstitution of P and Cl in Place of S**

*Summayya Kouser, S. R. Lingampalli, P. Chithaiah, Anand Roy, Sujoy Saha, Umesh V. Waghmare, and C. N. R. Rao**

Abstract: *Unlike cation substitution, anion substitution in inorganic materials such as metal oxides and sulfides would be expected to bring about major changes in the electronic structure and properties. In order to explore this important aspect, we have carried out first-principles DFT calculations to determine the effects of substitution of P and Cl on the properties of CdS and ZnS in hexagonal and cubic structures and show that a sub-band of the trivalent phosphorus with strong bonding with the cation appears in the gap just above the valence band, causing a reduction in the gap and enhancement of dielectric properties. Experimentally, it has been possible to substitute P and Cl in hexagonal CdS and ZnS. The doping reduces the band gap significantly as predicted by theory. A similar decrease in the band gap is observed in N and F co-substituted in cubic ZnS. Such anionic substitution helps to improve hydrogen evolution from CdS semiconductor structures and may give rise to other applications as well.*

It is customary to substitute metal ions in oxides, sulfides and other inorganic materials to bring about changes in their structure and properties. However, substitution of anions in these materials would be expected to bring about more significant changes in the electronic and optical properties. Thus, substitution of oxygen in colorless ZnO and TiO_2 by nitrogen changes the optical spectra giving rise to absorption in the visible region.[1,2] Nitrogen substitution in oxides gives rise to oxygen vacancies and this is prevented by co-substitution of N and F in oxides.[2,3] Such co-substitution changes the optical properties of ZnO and TiO_2 markedly rendering them orange and yellow colored, respectively, thereby reducing the band-gap of the oxides markedly. Accordingly, N, F-substituted ZnO and TiO_2 prepared recently show that the oxides exhibit visible-light induced reactivities.[2–4] In the light of the reports on the marked effects of co-substitution of N, F in oxides, it seemed important to explore whether the sulfide ion in metal sulfides can be substituted by phosphorus and chlorine. Such co-substitution by P and Cl in CdS and ZnS would be of great value in view of the highly desirable attributes of these important semiconductors. We have investigated the effects of co-substitution of P and Cl on these sulfides experimentally as well as theoretically. The results have been most rewarding in that there is a marked change in electronic structure on co-substitution of CdS and ZnS with P, Cl or N, F.

We first carried out first-principles density functional theoretical (DFT) calculations as implemented in the Quantum Espresso package[5] with interaction between ionic cores and valence electrons represented by means of ultrasoft pseudopotentials.[6] We have used two flavors of exchange correlation energy functionals: 1) generalized gradient approximation (GGA) of Perdew Burke–Ernzehof (PBE) and 2) local density approximation (LDA) of Perdew–Zunger (PZ) parameterized form, respectively.[7] A few calculations for estimation of band gap were carried out with a hybrid (HSE) functional, though it does not give very accurate estimates of band gaps.

Crystalline CdS occurs in cubic (c-CdS) and hexagonal wurtzite (h-CdS) structures belonging to $F\bar{4}3m$ (T_d^2) and $P6_3mc$ (C_{6v}^4) space groups, respectively, and the wurtzite phase is found to be more stable than c-CdS ($\Delta E = 2$ meV) in our calculations. Our estimates of the lattice constant obtained within GGA and LDA are within the typical DFT errors[8] (see Table SI in the Supporting Information). The electronic structures obtained within LDA and GGA are quite similar, and h-CdS exhibits a direct band gap of about 1.1 eV. Band gaps are typically underestimated in LDA- or GGA-based DFT calculations. An improved estimate of band gap using HSE functionals is 2.35 eV, in agreement with experimental value of 2.3 eV.[9] From the projected density of states (PDOS), we find that the energy bands immediately below the gap are constituted of p-orbitals of S and valence bands deeper in energy (about −8.5 to −7.5 eV) arise from d-orbitals of Cd. Conduction bands (just above the gap) are primarily contributed by s-orbitals of Cd, while the bands around 2–3 eV arise from p-orbitals of Cd (see Figure S1 a). Phonon spectrum of CdS confirms that the local structural stability of h-CdS (see Figure S1 b).

[*] S. Kouser, Prof. U. V. Waghmare
Theoretical Sciences Unit
Jawaharlal Nehru Centre for Advanced Scientific Research
Jakkur P.O., Bangalore 560 064 (India)
S. R. Lingampalli, Dr. P. Chithaiah, A. Roy, S. Saha, Prof. C. N. R. Rao
New Chemistry Unit, CSIR Centre of Excellence in Chemistry
International Centre for Materials Science and
Sheikh Saqr Laboratory
Jawaharlal Nehru Centre for Advanced Scientific Research
Jakkur P.O., Bangalore 560 064 (India)
E-mail: cnrrao@jncasr.ac.in

[**] S.K., S.R.L., and A.R. are greatful to CSIR, India for the research fellowship. S.K. is grateful to TUE-CMS, JNCASR for the computational facility. U.V.W. thanks DST, India for support through a JC Bose National Fellowship.

Supporting information for this article is available on the WWW under http://dx.doi.org/10.1002/anie.201501532.

We have considered three different kinds of anionic substitutions in h-CdS: 1) A, P substituted CdS (h-$CdS_{1-x}P_x$), 2) B, Cl substituted CdS (h-$CdS_{1-x}Cl_x$), and 3) A, B, with P, Cl co-substituted CdS (h-$CdS_{1-x-y}P_xCl_y$). To correlate our results with experiment, we have considered a $2\times1\times1$ periodic supercell containing 16 atoms: Cd_8S_8 with substitution of 1) one of the sulfur atoms with A amounting to 6.25%, 2) one of the sulfur atoms with B (6.25%), and 3) two of the sulfur atoms with A and B (12.5%). In the case of individual substitution of a p-type or a n-type atom at 6.25%, we have only one inequivalent configuration.[10] For co-substitution, there are many possible configurations corresponding to different of the ordering of A-and B-type atoms. We have employed the site occupancy disorder (SOD) technique which uses symmetry of the crystal to determine the inequivalent configurations.[10] We find three inequivalent configurations: A, B atoms present in different atomic planes and bonded to the same Cd atom (I), A, B atoms present in the same atomic plane and bonded to the same Cd atom (II) and A, B atoms bonded to different Cd atoms (III; see Figure S2). From their energies, we find that the configuration with A and B atoms occupying sites bonding to the same Cd atom but present in different planes to be the most stable one (see Table SII).

We first consider P and Cl for p-type and n-type doping, respectively. The change in the lattice parameters upon substitution with phosphorus and chlorine for sulfur is small (within about 1–2%). On the other hand, there are pronounced local structural distortions in the vicinity of the substitutional sites in the co-substituted CdS. The energetics of h-Cd_8S_7P, h-Cd_8S_7Cl, and h-Cd_8S_6PCl reveal that co-substitution with P and Cl is preferred over individual dopant substitutions with a lowering of energy by E_C = -1.94 eV per (P, Cl) pair, where E_C defines its relative stability [Eq. (1)].

$$E_C = E_{h-CdS_{1-x-y}A_xB_y} + E_{h-CdS} - E_{h-CdS_{1-x}A_x} - E_{h-CdS_{1-y}B_y} \quad (1)$$

Here, E_α (with α = h-$CdS_{1-x-y}A_xB_y$, h-CdS, h-$CdS_{1-x}A_x$ and h-$CdS_{1-y}B_y$) represents the total energy of the corresponding complex. It is the relative energy of bulk CdS and co-substituted CdS with respect to individually anion substituted CdS. For example, its negative value implies that co-substitution of P and Cl is energetically more favorable to P and Cl separately substituted in CdS. From bond valence analysis, Cd–P and Cd–Cl bond lengths are 2.49 and 2.98 Å, respectively, in Cd_8S_6PCl. Notably, these are 3% shorter and 9% longer, respectively, than the Cd–S bonds (2.57 Å) of bulk h-CdS, leading to a decrease in effective coordination number of Cd bonded with P and Cl in h-Cd_8S_6PCl to 3.31. These bond lengths are 4.2% shorter and 11.6% longer than average bond lengths of Cd–P (2.6 Å) and Cd–Cl (2.67 Å), respectively, in other Cd–P and Cd–Cl compounds reported in literature.[11]

Table 1: Comparison of electronic band gaps of Cd_8S_6AB with pristine CdS in hexagonal and cubic crystal structures.

System	Hexagonal E_g [eV]	Cubic E_g [eV]
CdS	1.11	1.00
Cd_8S_6PCl	0.53	0.97
Cd_8S_6NF	0.53	0.67
ZnS	2.00	2.07
Zn_8S_6PCl	1.33	1.88
Zn_8S_6NF	1.47	1.62

The electronic structure of h-Cd_8S_6PCl shows an isolated occupied band split from the rest of the valence bands (see Figure 1a), leading to a drastic decrease in band gap (ΔE_g = 0.58 eV, $E_g^{h-Cd_8S_6PCl}$ = 0.53 eV). To understand the nature of this isolated sub-band at the top of the valence band, we

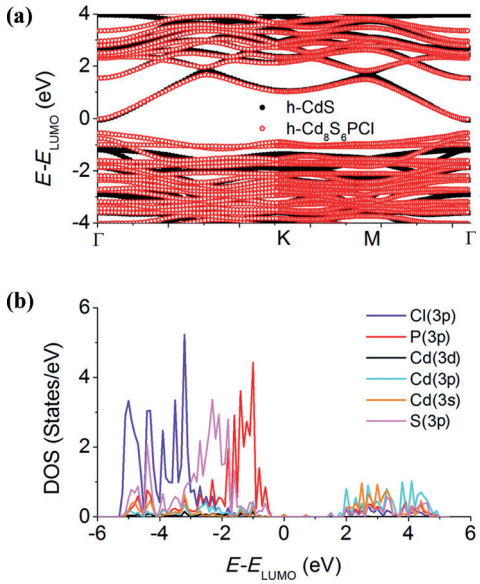

Figure 1. a) Electronic structure and b) projected density of states of h-Cd_8S_6PCl clearly reveal an isolated band emerging from 3p-orbitals of P at the top of valence band.

analyzed the density of electronic states of h-Cd_8S_6PCl by projecting them onto atomic orbitals and compared with bulk h-CdS. In bulk h-CdS, the valence band is constituted primarily of p-orbitals of S with a little mixing of d-orbitals of Cd. The uppermost valence band is most affected by phosphorus 3p states emerging as a sub-band with bandwidth of about 0.64 eV (See Figure 1b) in the gap. Analysis of the density of electronic states of h-Cd_8S_7P, h-Cd_8S_7Cl and h-Cd_8S_6PCl reveals that 1) 3p states of strongly electronegative Cl atoms are deep lying in energy (about −5–−2 eV) while those of the less electronegative P are concentrated at the top of the valence band, and 2) isolation of the sub-band of 3p states of P atom (in h-$CdS_{1-x-y}P_xCl_y$) from the rest of valence band becomes even more prominent on co-substitution with chlorine. The lowest energy conduction bands are essentially unaffected by P, Cl co-substitution and retain their Cd(3s) character.

The Born effective charge (BEC, $Z^*_{\alpha\beta}$) tensor is defined as the derivative of polarization P with respect to atomic displacemen [Eq. (2)],

$$Z^*_{i\alpha\beta} = \Omega \frac{\partial P\alpha}{\partial u_{i\beta}} \quad (2)$$

where i indexes an atom, α, β are cartesian indices, and Ω is the volume of the unit cell. Z^* gives the coupling between electric field (e.g., IR radiation) and the ionic lattice. The BECs of Cd ($Z^*_{xx,yy} = 2.23$, $Z_{zz} = 2.33$) and S ($Z^*_{xx,yy} = -2.27$, $Z^*_{zz} = -2.35$) are close to the nominal ionic charges of $+2$ and -2, respectively, indicating the ionic nature in h-CdS. In h-Cd_8S_6PCl, the BECs of P are ($Z^*_{xx} = -1.83$, $Z^*_{yy} = -1.73$, $Z^*_{zz} = -1.63$), while those of Cl are ($Z^*_{xx} = -1.82$, $Z^*_{yy} = -1.91$, $Z^*_{zz} = -1.91$). The anomaly in the BEC tensor of P is stronger compared to Cl, showing a higher chemical activity of P and relative inertness of Cl and confirming the mixed ionic/covalent and largely ionic nature of Cd–P and Cd–Cl bonds, respectively. Our calculations show an increase by 10–30 % in the electronic dielectric constant (ε^∞), another effect of the reduction in the electronic band gap on properties. In hexagonal CdS, the band gap decreases by 0.58 eV on substitution of P and Cl (Table 1).

Effects of anionic substitution in ZnS, which also exists in cubic and hexagonal structures (Figure 2), have been explored. Our estimates of the lattice constant for pristine ZnS are $a^{GGA}_{cubic} = 5.45$ Å and $a^{GGA}_{hexagonal} = 3.85$ Å, $c^{GGA}_{hexagonal} = 6.30$ Å, in good agreement with experiment.[12] The calculated band gaps of cubic and hexagonal phase of pristine ZnS are 2 and 2.07 eV, respectively. We consider co-substitution of (P, Cl) and (N, F) pairs for S in ZnS at the doping concentration of 12.5 %. On anionic co-substitution (12.5 % P, Cl), changes in the lattice parameters are similar to those in CdS counterpart. The changes in band gap of hexagonal and cubic phases are similar to those in Cd_8S_6PCl (see Figure 2). Thus, Zn_8S_6PCl shows a decrease in band gap of 0.67 and 0.19 eV, respectively, in the hexagonal and cubic phases (Table 1). The band gap decrease on N,F co-substitution is 0.53 and 0.45 eV in the hexagonal and cubic phases, respectively (Table 1).

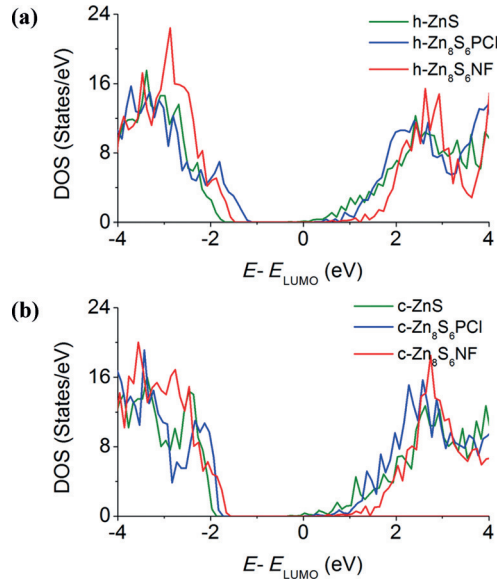

Figure 2. Comparison of density of states of Zn_8S_6AB with pristine ZnS for a) hexagonal and b) cubic crystal structures.

We have also examined the effect of substitution of other anions on structural and electronic properties of h-CdS. We consider co-substituted h-CdS with (N, F) pair at the same doping concentration. Here too, we find that co-substitution is preferred over the individual dopant substitutions with lowering of energy by 2.34 eV per (N, F). Similar to h-Cd_8S_6PCl, the isolated band arises from 2p-orbitals of less electronegative element (N) and the bands arising from more electronegative element (F) are much deeper in energy. The band gap decrease by N,F substitution is similar to the P, Cl substitution (Table 1).

The influence of the crystal structure on the effects of anion substitution on the electronic properties of CdS has been investigated by considering the cubic zinc-blended structure of CdS (see Figure S3). Our estimate of the lattice parameter obtained with GGA is $a = 5.93$ Å and is in good agreement with experimental value of 5.82 Å.[13] The decrease in band gap is however much smaller (about 0.03 eV) in the cubic phase of CdS compared to that in the hexagonal phase (Table 1).

We have been able to prepare CdS co-substituted with P and Cl by two methods. In the first method, CdS was treated with Cd_3P_2 and NH_4Cl at 400 °C in a nitrogen atmosphere. In the second method, CdS was heated with red phosphorus and NH_4Cl in two-steps (for details see the Experimental Section). The resulting products show the presence of P and Cl as determined by X-ray photoelectron spectroscopy (XPS). We show typical core level P 2p (133.3 eV) and Cl 2p (198.2 eV) spectra of a sample prepared by method 1 in Figure 3. The Cl 2p signal can be deconvoluted to four peaks corresponding to 2p 3/2 and 2p 1/2 (corresponding to substituted and interstitial Cl) with a spacing of 1.6 eV. The composition of this sample obtained was $CdS_{0.7}P_{0.14}Cl_{0.15}$. After P, Cl co-substitution, CdS assumes a brown color unlike pristine CdS which is yellow. The crystal structure of the undoped and doped CdS samples was hexagonal with unit cell parameters $a = 4.09$ Å, $c = 6.67$ Å and $a = 4.12$ Å, $c = 6.69$ Å, respectively. The electronic absorption spectrum of the P, Cl co-substituted CdS shows an extension of the absorption band edge to longer wavelengths. In Figure 4 a we compare typical absorption spectra of CdS and P, Cl co-substituted CdS. Pristine CdS shows a band gap of 2.3 eV where as the P, Cl co-substituted CdS shows a band gap around 1.8 eV, showing a shift of 0.5 eV. This large decrease in the band gap agrees with the theoretical prediction (≈ 0.5 eV) discussion earlier (Table 1). The sample of P,Cl co-substituted CdS prepared by the second method also had hexagonal structure ($a = 4.13$ Å, $c = 6.71$ Å). We show the electronic absorption spectrum of this sample with that of pristine CdS in Figure 4 b. We clearly see a decrease in the band gap.

We have been able to co-substitute sulfur with P and Cl in hexagonal ZnS as well. P, Cl co-substituted ZnS ($ZnS_{0.8}P_{0.1}Cl_{0.1}$) was obtained by the reaction of ZnS with Zn_3P_2 and NH_4Cl (see the Experimental Section). The co-substituted sample is slightly yellowish in colour. The crystal structure of P,Cl co-substituted ZnS is hexagonal with the unit cell parameters, $a = 3.82$ Å and $c = 6.25$ Å. P, Cl co-substituted ZnS shows the presence of P and Cl in XPS (Figure 3). Figure 5 a shows the absorption spectra of pristine ZnS and P,

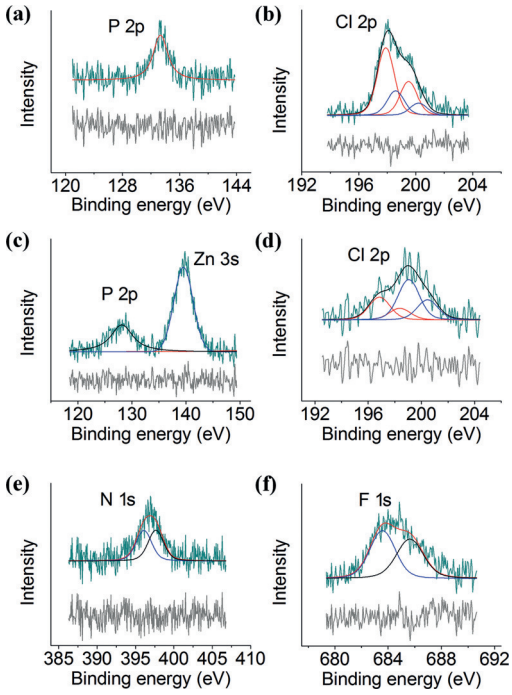

Figure 3. High-resolution XPS of a) P 2p and b) Cl 2p in P, Cl substituted CdS c) P 2p and d) Cl 2p in P, Cl substituted ZnS and e) N 1s and f) F 1s in N, F co-substituted ZnS.(Residual plots are given in gray color below the experimental data).

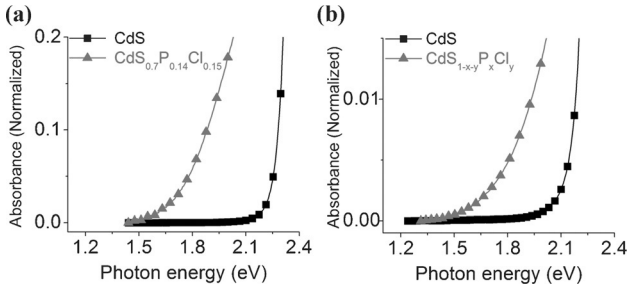

Figure 4. Comparison of electronic absorption spectra of pristine CdS and P and Cl co-doped CdS samples prepared by two methods.

Cl co-substituted ZnS. We see that the band gap of 3.5 eV in pristine ZnS decreases to 2.8 eV with shift of ≈0.7 eV. This shift is comparable with the theoretically predicted value of 0.67 eV (Table 1).

It has been possible to substitute N and F in place of S in cubic ZnS. N, F co-substituted ZnS was obtained by the reaction of ZnS with NH_3 and NH_4F (see the Experimental Section). The crystal structure of both pristine ZnS and N, F co-substituted ZnS was cubic with unit cell parameters of 5.41 and 5.39 Å, respectively. N, F co-substituted ZnS shows the presence of both N and F, in the XPS. In Figure 3, we show the N 1s spectra. The N 1s core level XPS signal can be deconvoluted into two peaks located at 396.0 and 397.7 eV. The peak at 396.0 eV is assigned to N 1 s as in S-Zn-N, and the peak located at 397.7 eV is assigned to N 1s in surface adsorbed NH species. The F 1s core level signal can be deconvoluted to two peaks located at 683.5 and 685.7 eV of which the one at 383.5 eV is assigned to F 1s in S-Zn-F

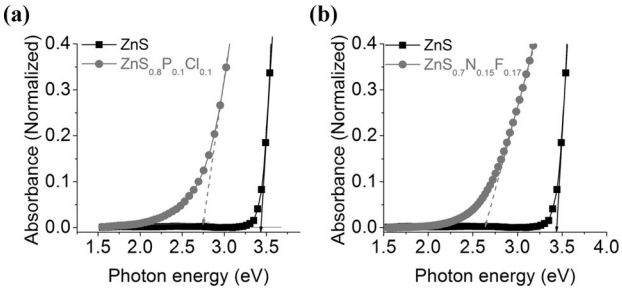

Figure 5. Comparison of electronic absorption spectrum of ZnS with that of a) P, Cl substituted ZnS and b) N,F substituted ZnS.

(Figure 3).[2] The composition of the N, F co-substituted ZnS was determined as $ZnS_{0.7}N_{0.15}F_{0.17}$. The absorption spectra of pristine ZnS and $ZnS_{0.7}N_{0.15}F_{0.17}$ are compared in Figure 5b. The latter is yellow in color. The absorption edge of $ZnS_{0.7}N_{0.15}F_{0.17}$ shows a red shift from 3.5 eV to 2.7 eV, the magnitude of the shift being 0.8 eV. This is to be compared with the theoretically predicted shift of 0.45 eV.

We have carried out a preliminary study of photocatalytic hydrogen generation using P, Cl substituted CdS. In Figure 6, we show the hydrogen evolution of CdS/Pt and $CdS_{1-x-y}P_xCl_y$/Pt under visible-light irradiation in the presence of Na_2S-Na_2SO_3 as sacrificial agents. $CdS_{1-x-y}P_xCl_y$/Pt, prepared by the second method exhibits an enhanced hydrogen evolution activity compared to that of CdS/Pt with a yield of 3.3 mmol h^{-1} g^{-1}. It would be of value to carry out further studies of P,Cl and N,F doped CdS and ZnS.

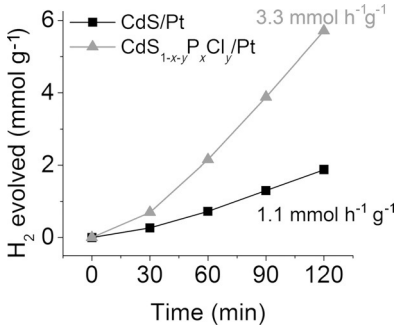

Figure 6. Visible-light-induced hydrogen evolution by CdS/Pt and $CdS_{1-x-y}P_xCl_y$/Pt as a function of time in presence of Na_2S-Na_2SO_3.

In conclusion, CdS and ZnS become p- and n-type semiconducting with the substitution of the phosphorus (or nitrogen) and chlorine (or fluorine), respectively. Anionic co-substitution is energetically preferred over individual substitutions by more than 1.5 eV/atom, and P, Cl (or N, F) atoms preferentially occupy sites bonding to Cd or Zn in the lowest energy configuration. The reduction in band gap in P, Cl co-substituted CdS and ZnS arises from the emergence of an isolated sub-band at the top of the valence band which is primarily contributed by the less electronegative trivalent anion like P (or N). Bands of the more electronegative Cl and F anions lie deep in energy well below the valence band. Changes in the electronic band gap are predicted to be more pronounced in the hexagonal crystal structure for P, Cl co-

substituted CdS and ZnS. Effects of anionic co-substitution on the electronic structure are sensitive to the crystal structure as well as to the dopants. We have been able to prepare P, Cl co-substituted CdS and ZnS in hexagonal structures and characterized them adequately. They both show marked decrease in band gaps, close to the shifts predicted by theory. N, F co-substituted ZnS in the cubic structure shows a large decrease in the band gap as predicted. We believe that properties of P, Cl (N, F) co-substituted CdS and ZnS may indeed be useful in many situations.

Experimental Section

P, Cl co-substituted CdS was obtained by two procedures. In one method, Cd (3 mmol) and red phosphorus (2.5 mmol) were ground uniformly and made as a pellet. The sample was heated at 400 °C for 2 h in nitrogen atmosphere in a tube furnace. The resulting product (Cd_3P_2) was ground uniformly and used for further studies. CdS (2 mmol), Cd_3P_2 (0.1 mmol) and NH_4Cl (0.6 mmol) were ground uniformly and made as a pellet. The pellet was heated at 400 °C for 6 h in nitrogen atmosphere in a tube furnace. After the reaction, the sample was allowed to cool down to room temperature naturally. The resulting sample ($CdS_{1-x-y}P_xCl_y$) was ground uniformly and used for further characterization.

In the second method, CdS (2 mmol), red phosphorus (2 mmol) and NH_4Cl (1 mmol) were ground uniformly and made as a pellet. The pellet was heated at 350 °C for 2 h in nitrogen atmosphere in a tube furnace. After the reaction, sample was allowed to cool down to room temperature naturally. The resulting sample was ground uniformly and again made as a pellet. This sample was heated at 400 °C for 1 h in nitrogen atmosphere. After the reaction, the sample was allowed to cool down to room temperature naturally. The resulting sample ($CdS_{1-x-y}P_xCl_y$) was ground uniformly and used for further characterization.

P, Cl co-substituted ZnS was prepared by the following procedure. Zn (3 mmol) and P (2.5 mmol) were ground uniformly and made as a pellet. The pellet was heated at 350 °C for 2 h followed by heating at 400 °C for 2 h in nitrogen atmosphere in a tube furnace. After the reaction, the resulting product (Zn_3P_2) was ground uniformly and used for further studies. ZnS (3 mmol), Zn_3P_2 (0.15 mmol) and NH_4Cl (0.9 mmol) were uniformly ground and made as a pellet. The pellet was heated at 600 °C for 6 h in nitrogen atmosphere in a tube furnace. After the reaction, the temperature was allowed to cool down to room temperature naturally. The resulting product ($ZnS_{1-x-y}P_xCl_y$) was ground uniformly and characterized.

N, F co-substituted ZnS was obtained as follows. ZnS (3 mmol) and NH_4F (40 mmol) were uniformly ground and transferred to a ceramic boat and placed in a tube furnace. The sample was heated at 600 °C for 2 h in a continuous flow of ammonia. After the reaction the temperature was allowed to cool down to room temperature naturally. The resulting product was ground uniformly and characterized.

The X-ray diffraction patterns (XRD) of the products were recorded with Bruker D8 Diffraction System using a Cu K_α source ($\lambda = 0.154178$ nm). UV/Vis absorption spectra were taken with PerkinElmer Model Lambda 750 spectrometer. In the photocatalytic activity study, 20 mg of the photocatalyst (1 mol% Pt was deposited by the reduction of H_2PtCl_6 with $NaBH_4$) was dispersed in a 75 mL of water containing 0.1 M Na_2S and 0.1 M Na_2SO_3 in a quartz cell. The solution was illuminated with 450 W Xe arc lamp (working at 400 W) (New Port, 6279NS, Ozone-free) fitted with water (IR) filter (New Port). A 395 nm cut-off filter was employed to remove the UV fraction leaving behind the visible fraction of light (> 395 nm). The H_2 evolved was quantified using gas chromatography (PerkinElmer, Clarus 580 GC) equipped with TCD detector.

Computational details

In our DFT calculations,[5–7] we have employed a plane-wave basis truncated with energy cutoffs of 30 Ry and of 180 Ry in representation of wave functions and charge density, respectively. Within periodic boundary conditions, suitable supercells of CdS and ZnS are used to model the desired concentration of anion dopants. We use uniform mesh of $12 \times 12 \times 9$ and $12 \times 12 \times 12$ k-points in sampling integrations over the Brilloiun zones of hexagonal and cubic structures, respectively, and smear the discontinuity in the occupation numbers of electronic states using the Fermi-Dirac distribution with smearing width (k_BT) of 0.04 eV. We have relaxed the structure to minimize energy until the Hellman–Feyman forces are less than 0.03 eV $Å^{-1}$ in magnitude. Since the band gap is underestimated in DFT-LDA calculations, we use hybrid density functionals based on a screened Coulomb potential for Hartree–Fock exchange (HSE), and obtain more accurate estimates of the band gap of a few of these compounds.

Keywords: co-substitution · electronic structure · photocatalysis · semiconductors · X-ray photoelectron spectroscopy

How to cite: *Angew. Chem. Int. Ed.* **2015**, *54*, 8149–8153
Angew. Chem. **2015**, *127*, 8267–8271

[1] H. Qin, W. Li, Y. Xia, T. He, *ACS Appl. Mater. Interfaces* **2011**, *3*, 3152–3156; Z. Zhang, Z. Luo, Z. Yang, S. Zhang, Y. Zhang, Y. Zhou, X. Wang, X. Fu, *RSC Adv.* **2013**, *3*, 7215–7218.
[2] R. Saha, S. Revoju, V. I. Hegde, U. V. Waghmare, A. Sundaresan, C. N. R. Rao, *ChemPhysChem* **2013**, *14*, 2672–2677; S. R. Lingampalli, C. N. R. Rao, *J. Mater. Chem. A* **2014**, *2*, 7702–7705.
[3] N. Kumar, U. Maitra, V. I. Hegde, U. V. Waghmare, A. Sundaresan, C. N. R. Rao, *Inorg. Chem.* **2013**, *52*, 10512–10519; N. Kumar, J. Pan, N. Aysha, U. V. Waghmare, A. Sundaresan, C. N. R. Rao, *J. Phys. Condens. Matter* **2013**, *25*, 345901.
[4] H. Irie, Y. Watanabe, K. Hashimoto, *J. Phys. Chem. B* **2003**, *107*, 5483–5486; G. Liu, H. G. Yang, X. Wang, L. Cheng, J. Pan, G. Q. Lu, H.-M. Cheng, *J. Am. Chem. Soc.* **2009**, *131*, 12868–12869.
[5] P. Giannozzi, S. Baroni, N. Bonini, M. Calandra, R. Car, C. Cavazzoni, D. Ceresoli, G. L. Chiarotti, M. Cococcioni, I. Dabo, A. D. Corso, S. d. Gironcoli, S. Fabris, G. Fratesi, R. Gebauer, U. Gerstmann, C. Gougoussis, A. Kokalj, M. Lazzeri, L. Martin-Samos, N. Marzari, F. Mauri, R. Mazzarello, S. Paolini, A. Pasquarello, L. Paulatto, C. Sbraccia, S. Scandolo, G. Sclauzero, A. P. Seitsonen, A. Smogunov, P. Umari, R. M. Wentzcovitch, *J. Phys. Condens. Matter* **2009**, *21*, 395502.
[6] D. Vanderbilt, *Phys. Rev. B* **1990**, *41*, 7892–7895.
[7] J. P. Perdew, K. Burke, M. Ernzerhof, *Phys. Rev. Lett.* **1996**, *77*, 3865–3868; J. P. Perdew, A. Zunger, *Phys. Rev. B* **1981**, *23*, 5048–5079.
[8] S.-H. Wei, S. B. Zhang, *Phys. Rev. B* **2000**, *62*, 6944–6947.
[9] L. A. Silva, S. Y. Ryu, J. Choi, W. Choi, M. R. Hoffmann, *J. Phys. Chem. C* **2008**, *112*, 12069–12073.
[10] R. Grau-Crespo, S. Hamad, C. R. A. Catlow, N. H. d. Leeuw, *J. Phys. Condens. Matter* **2007**, *19*, 256201.
[11] R.-Q. Zhu, *Acta Crystallogr. Sect. E* **2011**, *67*, m1416–m1416; M. S. Bharara, C. H. Kim, S. Parkin, D. A. Atwood, *Polyhedron* **2005**, *24*, 865–871.
[12] S. Desgreniers, L. Beaulieu, I. Lepage, *Phys. Rev. B* **2000**, *61*, 8726–8733.
[13] H. Derin, K. Kantarlı, *Surf. Interface Anal.* **2009**, *41*, 61–68.

Received: February 16, 2015
Published online: June 1, 2015

